Evaluation of short-circuited electrodes in combination with dark fermentation for promoting biohydrogen production process

D. Truong, Frédérique Changey, Emmanuel Rondags, Xavier Framboisier, Mathieu Etienne, Emmanuel Guedon

Evaluation of short-circuited electrodes in combination with dark fermentation for promoting biohydrogen production process

Delphine Truong[1,2], Frédérique Changey[2], Emmanuel Rondags[1], Xavier Framboisier[1], Mathieu Etienne[2 *], Emmanuel Guedon[1 *]

[1] Université de Lorraine, CNRS, LRGP, 54500 Nancy, France

[2] Université de Lorraine, CNRS, LCPME, 54000 Nancy, France

Abstract

Short-circuited electrodes, in combination with dark fermentation, were evaluated in a biohydrogen production process. The system is based on an innovative design of a non-compartmented electromicrobial bioreactor with a conductive tubular membrane as cathode and a graphite felt as anode. In particular, the electrode specialization occurred when the bioreactor was inoculated with manure as the whole medium and when a vacuum was applied in the tubular membrane, for allowing continuous extraction of gaseous species (H_2, CH_4, CO_2) from the bioreactor. This specialization of the electrodes as anode and cathode was further confirmed by microbial ecology analysis of biofilms and by cyclic voltammetry measurements. In these experimental conditions, the potential of the electrochemical system (short-circuited electrodes) reached values as low as -320 mV vs. SHE, associated with a significant bioH_2 production. Moreover, a higher bioH_2 production occurred and a potential of the electrochemical system as low as -429 mV vs SHE was temporarily observed, when additional heat treatments of the whole manure were applied in order to remove methanogen microorganisms (i.e., hydrogen consumers). In the bioreactor, the higher production of bioH_2 would be promoted by electrofermentation from the current flow observed between short-circuited anode and cathode.

Keywords

Biohydrogen, short-circuited electrodes, electrochemical snorkel, dark fermentation

*Corresponding author. Université de Lorraine, CNRS, LRGP, 54500 Nancy, France. Email adress: emmanuel.guedon@univ-lorraine.fr (E. Guedon)
Université de Lorraine, CNRS, LCPME, 54500 Nancy, France. Email adress; mathieu.etienne@cnrs.fr (M. Etienne)

1. Introduction

In the context of global warming, energy transition is both a societal and an environmental challenge. With the transition out of fossil energy, development of renewable energy is one of the main solutions to make possible this transition. In recent years, hydrogen has been seen as a credible carbon-free energy resource, used either for direct combustion or in a fuel cell. However, the production of hydrogen is currently of petrochemical origin, thanks to processes that are cheap but that have the disadvantage of being non-renewable and polluting, and therefore generating large amounts of CO_2 (Mosca et al. 2020). As a result, efforts have been made to reduce both costs and CO_2 emissions, by developing alternatives using e.g. electrolyzers or, to a lesser extent, biological processes using microbial technologies (Ghimire et al. 2015).

One of the most studied microbial methods is based on dark fermentation (DF), and more specifically on the capability of specific microorganisms to produce biohydrogen ($bioH_2$) (Ghimire et al. 2015; Renaudie et al. 2021; Oh et al. 2004; Wang et al. 2018). In these microorganisms, mainly strict anaerobe species such as *Clostridium sp.*, carbon substrates are fermented to provide energy, which consequently generates an electron flux that can be used by a hydrogenase activity to produce $bioH_2$ (Saint-Amans et al. 2001). In fact, with the use of specific co-factors, this enzyme can catalyze both the production and/or the consumption of H_2, depending on different parameters such as H_2 partial pressure (P_{H2}) (Mizuno et al. 2000) and the redox environment or pH (Guo et al. 2010). This enzyme is mainly found in a large range of microorganisms such as *Clostridium* species, present in mixed culture dedicated to dark fermentation for $bioH_2$ production (Barca et al. 2016; Morsy 2017; Zagrodnik et Łaniecki 2017). During this process, H_2 pressure (i.e. P_{H2}), can be reduced in order to favor H_2 production by using a gas flow as a carrier or using vacuum directly in the headspace of the bioreactor or through a liquid/gas membrane (Renaudie et al. 2021; Lee et al. 2012).

As an alternative to DF, Microbial Electrolysis Cell (MEC) have been evaluated for hydrogen production (Lalaurette et al. 2009; Mohan et Pandey 2013; Jeremiasse, Hamelers, et Buisman 2010). This approach is based on microorganisms that can exchange electrons with the extracellular environment, and more specifically with electrodes. In fact, electroactive microorganisms can be either exoelectrogenic or electrotrophic, according to their capacity of giving/receiving electrons to/from the environment, respectively (Logan et al. 2019). MEC can use the electron flow extracted from organic substrate oxidation at the bioanode to induce reactions of interest at the cathode, *e.g.* $bioH_2$ production. The production of $bioH_2$ is however

thermodynamically unfavorable (Cheng et Logan 2007; Zaybak et al. 2013; Reeve et al. 2017). and it is necessary to add at least a potential of 0.13 V between the microbial anode and the cathode (biotic or abiotic) to overcome this thermodynamic barrier. The potential applied in MEC for bioH_2 production is significantly lower than the one needed for water splitting when water is oxidized in place of organic matter, but the microbial electrolysis still consumes energy for H_2 production. This limitation has been somehow overpassed by microbial bioH_2 producers from the environment that have developed during their evolution biochemical pathways to produce this gas despite the unfavorable potential difference between NADH/NAD^+, H^+ and H^+/H_2 redox couples (-320 and -414 mv vs. SHE respectively). The purpose of this study was to evaluate a strategy to promote bioH_2 without the external energy input requested in microbial electrolysis.

According to the literature, bioH_2 recovery can reach 33% using DF and 50 to 90 % using 0.6 V applied for MEC, the highest recovery being observed with acetate and lactate as the substrate (Cheng et Logan 2007). This value can be difficult to reach in complex media such as in organic waste because of the complex microbial population present inside. To reach the highest bioH_2 production from organic wastes, combining DF and MEC has to be considered (Lalaurette et al. 2009; Guo, Prévoteau, et Rabaey 2017; Katuri et al. 2014; Werner et al. 2016; Wang et al. 2013). In fact, bioH_2 production on its highest rate on MEC is done using substrates that are found in fermentation such as volatile fatty acid (VFA, i.e. acetate, butyrate…) instead of glucose substrate for which bioH_2 recovery could only reach 71% in MEC operated at 0.6 V (Cheng et Logan, 2007). In initial experiments that involved the integration of DF and MEC technologies, the production of bioH_2 was achieved through a sequential two-step process. In the initial phase of DF, the oxidative breakdown of organic substrates within the medium resulted in the generation of hydrogen, concurrently with the production of VFA. In a subsequent stage, these VFA generated in the DF process were transported to an electrochemical cell and subjected to oxidation by an electroactive bacteria biofilm within the anodic chamber (Lalaurette et al. 2009). It has been demonstrated that the combination of these two methods led to an increase in bioH_2 production (Lalaurette et al. 2009; Liu et al. 2012; Moreno et al. 2015). For example, Lalaurette et al., demonstrated that employing effluents from cellobiose fermentation to supply a MEC resulted in achieving a hydrogen yield of 9.95 $mol_{H2}/mol_{glucose}$ while DF alone yielded only 1.64 $mol_{H2}/mol_{glucose}$ (Lalaurette et al. 2009). This

difference can be attributed to the various oxidation degrees of organic components of the medium.

The combination of the two methods into a single step process was later considered. In order to reduce internal resistance present in MEC, the two electrodes chamber could be combined by implementing electrodes closer to each other without separation. In addition, the global system could be additionally simplified by using conductive membranes, such as nickel based hollow fiber, making them able to work either as a cathode and for gas extraction (Katuri et al. 2014; Werner et al. 2016). However, some important experimental conditions are not always easy to set up, depending mostly on microorganism optimal cultures. As an example, the optimal pH of fermentative microorganisms in DF usually ranges between 5 to 6 (Guo et al. 2010) while it is around 7 for electroactive bacteria in MEC (Patil et al. 2011) and some compromise values had to be established. Another difficulty is related to H_2 consumer microorganisms that are naturally present in the complex environment such as manure or waste-based media.

Apart from MEC, DF and any combination of these two processes, another concept, the microbial electrochemical snorkel involving short-circuited electrodes (SCE; anode and cathode) emerged recently in the area of microbial electrochemistry (Erable et al. 2011). SCE do not produce nor consume electricity but permits to connect efficiently separated electromicrobial processes and was shown to be efficient for the passive water treatment by promoting organic matter oxidation (Hoareau et al. 2023), nitrate removal (Rogińska et al. 2021, 2023) or metal recovery (Mitov et al. 2021, 2022; Hubenova et al. 2023). The main interest of SCE lies in its simplicity, not requiring external power sources to run the process. For electrochemical studies, the short-circuit can be analyzed with zero resistance amperometry, allowing identification of the anodic and the cathodic sides of the electrochemical system and measurement of both the current flowing between the two short-circuited electrode and the potential of the system versus a defined reference electrode (Rogińska et al. 2021).

Hence, the purpose of this study was to evaluate the possibilities offered by short-circuited electrodes in combination with DF for bioH_2 production, considering the mechanism of electrofermentation. To this end, experiments were carried out in a non-compartmentalized bioreactor inoculated with manure as the whole medium, inside which a graphite felt was used as a bioanode while a conductive tubular membrane was used as both biocathode and for gas extraction. First, the experimental design has been optimized to achieve the lowest electrode potential, close to -300 mV *vs* SHE, in order to promote the production of microbial bioH_2,

monitored with gas chromatography. Subsequently, the electrochemical specialization of the electrodes on which biofilms developed was characterized and monitored during the process, using electrochemical measurements and metagenomic analyses of microbial communities.

2. Material and methods

2.1. Experimental design

A 5 liters bioreactor was used for all experiments. The electrochemical device was composed of three electrodes, the working electrode was a carbon-based silicone tubular membrane (Getelec, France), the counter electrode was made with a piece of graphite felt (GFD 4.6EA, SGL, Germany) and the reference electrode was an Ag/AgCl/KCl 1M. A porous separator, made with a high-density polypropylene geotextile membrane, was implemented at the surface of the graphite felt, between the two electrodes to prevent direct contact. Electrochemical analysis was done with a VSP-3e potentiostat (Biologic, France). Following a previous report (Rogińska et al. 2021), the electrochemical noise mode of the EC-Lab software (Biologic, France) was used to short-circuit the graphite felt and the conductive tubular membrane while the current as well as the potential of the whole system were measured between the two electrodes. All potentials were then recorded versus standard hydrogen electrode (SHE) by adding 240 mV to the measured values. The current density was calculated according to the geometric surface area of the electrodes. Potential and current values were collected every minute. Open circuit voltage (OCV) and cyclic voltammetry (CV) at 1mV/s were measured on individual electrodes.

Three designs of the bioreactor process were tested during this study (Figures 1 to 3). For all experiments, the tubular membrane was connected to an insulated stainless-steel tube. The graphite felt was connected to a stainless-steel rod and through a butyl septum in the headplate of the bioreactor in order to avoid any oxygen entry.

In the first design of the bioreactor process, a tubular membrane (inner diameter x outside diameter x length of 3.5 mm x 5.5 mm x 80 mm) was connected to two stainless steel tubes inside which 0.11 mL/min of air or N_2 were used as gas carrier for gas extraction. The graphite felt piece (80mm x 85 mm x 4 mm) was placed at two-thirds in the organic medium and one-third in the headspace of the reactor.

In the second design of the bioreactor, the graphite felt piece (a 160 mm disc in diameter with 5 mm in thickness) was placed at the bottom of the reactor whereas the tubular membrane did

not change compare to the first design. A flow of N_2 at 0.11 mL/min inside the tubular membrane was used as gas carrier for gas extraction

In the third design of the bioreactor, the graphite felt piece (a 160 mm disc in diameter with 5 mm in thickness) was placed at the bottom of the reactor and a 80 mm tubular membrane was closed in one extremity with a 20 mm stainless steel stem. Instead of a gas carrier, a vacuum of 80 kPa was applied inside the tubular membrane, using membrane pump (N86 Labort, KNF, Germany).

In this final experimental design of the bioreactor, a vacuum of 80 kPa was applied continuously for long term electrochemical and gas analyses.

2.2. Culture conditions

Cultures were inoculated using manure from either the methanizers of Methanason (Einville-au-Jard, France) or La Bouzule farm (Nancy, France) as the whole medium. The two methanizers were feed with the same organic wastes, were associated and were actives for dark fermentation. The manure collected at t_0 was directly introduced into the bioreactor. A first vacuum was made through the membrane, in the medium and in the headspace to remove all O_2 present in the bioreactor. Then, N_2 was, used to fill the membrane and the headspace in order to limit O_2 entry when the vacuum was stopped. Electrochemical and daily gas analyses started when vacuum was applied to the membrane. After the system reached potential and current equilibrium values, two successive heat treatment at 121 °C were done to the medium for electrochemical and gas analysis.

2.3. Gases analysis

H_2 and CH_4 from the membrane and headspace of the reactor were analyzed online with a Micro Gas chromatography (microGC fusion, Chemlys) equipped with two Thermal Conductivity Detector (TCD, columns A and B) were used for gas composition analysis with argon as carrier gas on the detector A and helium as carrier gas for the detector B. The A and B column were set at 80 °C and 75°C respectively. The detector was set 70 °C.

2.4. Electrofermentation coefficient

Electrofermentation coefficient (η_{EF}) was calculated following the equation proposed by Moscoviz et al., 2016, using the charge transferred (Q_{e^-}) and the total charged product (Q_p):

$$Q_{e^-} = \int I \mathrm{d}t \quad (1)$$

Where I is the electric current recorded over a time.

$$Q_p = n_p \times N_p \times F \quad (2)$$

With n_p the number of moles of the product, N_p the number of moles of electrons available per mole of product which can be calculate using this formula: $N(C_aN_bO_cH_d) = 4a - 3b - 2c + d$, and F the Faraday constant (96 485 C/mol).

$$\eta_{EF} = Q_{e^-}/Q_p \quad (3)$$

The value of the coefficient is always positive. If the value is >1, the system may be close to a microbial fuel cell that a significant current density and the system is able to drive a bioH_2 electrosynthesis. If the coefficient is comprised between 0 and 1, the electron present in the electric circuit could not contribute directly to H_2 production and the electrosynthesis may not be the main reaction in the electrochemical system (Moscoviz et al. 2016).

2.5. Microbial community analysis

DNA extraction and amplicon sequencing. At the beginning and the end of each experiment, manure was sampled for global microorganism community analysis. Biofilm samples, from both the felt (anode) and tubular membrane (cathode) surfaces were collected at the end of the experiment. Total DNA extraction from biofilm and manure were made in 50 mL of phosphate buffer following two steps. First of all, an ultrasound treatment was made at 45 kHz for 10 min, using an Ultrasonic Cleaner (VWR, France). Then, each electrode was scratched using a scalpel in order to remove biofilm from their surface. All biofilm and manure samples were then centrifuged at 5 500 G for 10 min and supernatants were removed before storing them at -80 °C. DNA extraction from all supernatants was performed using DNeasy PowerSoil Pro (Qiagen, Hilden, Germany) according to the manufacturer recommendations for water and biofilm samples, respectively. DNA were eluted in 100 µL of elution buffer and their concentration were measured using a QuBit4 Fluorometer (Invitrogen, Waltham, USA). In addition, purity of extracted DNA was assessed by measuring both 260/280 nm and 260/230 nm ratios with a NanoDrop spectrophotometer (Thermo Scientific, Waltham, USA). DNA was stored at 4°C until further analysis. 16S rDNA V3-V4 region sequencing was performed by Novogene (Cambridge, United Kingdom) at PE250 an Illumina Novaseq (Illumina, United States).

Bioinformatic analysis. Data were subsequently imported into the FROGS pipeline (Find Rapidly OTU with Galaxy Solution) implemented on a galaxy instance (v.2.3.0) (http:// sigenae-workbench.toulouse.inra.fr/galaxy/) (Escudié et al., 2018). After a quality control, 16S paired-end sequences were merged into contigs with VSEARCH (Rognes et al., 2022). Sequences were dereplicated before being clustered using SWARM algorithm (v.2.1.5) (Mahé et al., 2022) with a first denoising step using an aggregation distance equal to 1 and a second one equal to 3. Chimera were removed using VSEARCH (Rognes et al., 2022). Filters were applied to remove clusters that are not present in at least 3 samples or with an abundance below a 0.005% threshold (Bokulich et al., 2013). The taxonomic assignation of each OTU was performed using the BLAST tools against (Camacho et al., 2009) the database SILVA 132 16S (Pruesse et al., 2007). Phyloseq (1.26.1) R package was used to identify community composition analysis, to normalize and to generate α-diversity indexes (richness and evenness) after a rarefaction curve using the transform counts method (McMurdie and Holmes, 2013).

*Statistical analysis.*All statistical analyses were carried out using R software version 2023.06.1 (R Development Core Team, http://www.R-project.org). We first compared α-diversity indexes to summarize the structure microbial communities with respect to its richness (number of Amplicon Sequence Variant (ASV)) and Simpson index (distribution of abundances of the OTU) with phyloseq (1.44.0) (McMurdie and Holmes, 2013). A t-test was performed on richness and shannon for pairwise comparisons using "Microbiome" package. The β-diversity, to assess the degree of community differentiation, was estimated using multivariate analyses. The dissimilarities (Weighted Unifrac distances) among treatments were assessed using Principal Coordinate Analysis (PCoA). After testing the multivariate homogeneity of group dispersions, permutational analysis of variance (PERMANOVA) (adonis" function on vegan 2.6-4 R package) was performed to test for significant differences in sample clustering patterns across sampling points (9999 permutations). Plots were drawn using the R packages ggplot2 (3.4.3) 1). Heatmaps were plotted with R package ampvis2 (2.8.6) (Andersen et al., 2018).

2. Results and discussion

3.1. Reactor designs

Preliminary experiments were carried out in order to design a reactor that could be favorable to bioH_2 production by simply short-circuiting an anode to a relatively smaller cathode, in a liquid manure coming from methanizers as the biological component. In such conditions, low

potentials and current flow from the larger anode to the smaller cathode were expected. In this study, the large anode was made with a piece of graphite felt whereas the smaller cathode was designed with a conductive tubular membrane that allows extraction of the produced gases, either by flowing N_2 or by applying a limited vacuum to the membrane in order to specialize electrodes. The main criteria in this first series of experiments were the measurement of the current, the characterization of the direction of this electron flow (current must be negative at the tubular membrane side, the cathode), and the potential reached by the system with manure while the current was flowing between anode and cathode. In this configuration of the process, the potentiostat was only used to monitor the resulting potential and was never used for applying any external potential and forced current flow.

A first process configuration is reported in Figure 1. In this experiment, a carrier gas (N_2) was used through the internal tube of the conductive membrane located inside the manure. A graphite felt piece was introduced as represented in Figure 1A, a larger part being in the organic matter, and a smaller emerged in the headspace of the reactor where electrical connections were established. The experiment was initiated by flowing air inside the membrane, while N_2 was injected in the headspace of the bioreactor. The two electrodes, i.e. the conductive tubular membrane and the graphite felt, were short-circuited using a special measurement mode offered by the potentiostat that allowed implementing a zero-resistance between them. As a result, an electrical current between these electrodes and the potential of the whole system were measured (Figure 1B).

In these experimental conditions, the potential was close to -30 mV vs SHE and the current reached -5 µA/cm² at the tubular membrane that behaved thus as a cathode when air was flowing through it (Figure 1B). Air contains 20 % oxygen that was readily reduced at the membrane, and at this potential, it could result from either abiotic reduction, or reduction through biofilm catalysis. Flowing N_2 inside of the tubular membrane drastically changed the experiment and the current became positive, reaching 8-9 µA/cm². Hence, the membrane switched from a cathode to an anode and the origin of this positive current could result from the oxidation of organic matter at the membrane surface, due to microorganism activities. Microbial electrodes that can rapidly switch from bioanodic to biocathodic behavior have been already reported in the literature (Rozendal et al. 2008; Jeremiasse et al. 2010). However, the potential of the system did not change dramatically during the experiment and only oscillated between -20 to -50 mV in the presence of air to -30 and -50 mV in the presence of N_2. In this

experiment, the lowest potential was observed when the membrane was behaving as an anode, when purged with N_2, but potential measurements were very far from what was expected, i.e. a low equilibrium potential close to -300 mV vs SHE. Higher potentials were obtained if one of the electrode is contaminated by oxygen, as already reported (Reeve et al. 2017). In our study, the hypothesis that the headspace of the reactor was not completely free of oxygen was privileged. Therefore, the first design of the reactor that involved a wetted graphite felt, largely exposed to the headspace, probably switched from an anodic to a cathodic behavior since this structure can canalize organic matter components by capillarity, that can consequently be in contact and react with oxygen traces and thus limiting the bioH_2 production (Hoareau et al. 2023).

To prevent such exposure to oxygen traces, the graphite felt electrode was more deeply immersed at the bottom of the reactor (see Figure 2A), and covered with an insulating porous separator to prevent any uncontrolled short-circuit with the tubular membrane. In addition, N_2 was flowed in the tubular membrane in order to extract gases produced at the vicinity of the surface membrane where dark fermentation occurred.

Figure 2B reports the behavior of the new configuration of the system as described above, when the two electrodes were short-circuited. The initial potential was relatively high, around -50 mV vs SHE before to gradually decrease to -250 mV within 25 hours, which was close to the maximum potential that bacteria can reach in anaerobic conditions, -300 mV (Cheng et Logan 2007). In the same time, an unstable positive current, starting from 5 µA/cm², decreased to a negative and stable value of -0.28 µA/cm². The large current observed during the first hours was probably due to the presence of oxygen traces in the manure due to the inoculation from methanizer into the bioreactor that were gradually consumed until exhaustion. Whereas the final measured current was relatively low but stable, the electron flow was consistent with the membrane behaving as a cathode. After 100h, when the N_2 flow was stopped, some oxygen traces probably entered again into the tubular membrane. The current remained negative but a rapid switch in current was observed, from -0,28 µA/cm² to -9 µA/cm², associated to a rapid switch of the potential from -250 mV to -100 mV. In such experimental system equipped with short-circuited electrodes, a higher current is usually associated with a higher potential of equilibrium (Rogińska et al. 2021). Moreover, it was assumed that the presence of oxygen necessarily pushed the redox potential of the whole system to higher values. Flowing N_2 again through the membrane allowed a rapid recovery of the low potential and the current diminished back to about -3µA, and the tubular membrane behaved continuously as a cathode.

In this second design of the bioreactor, the conductive tubular membrane could behave as a robust cathode when short-circuited with a larger piece of graphite felt that behaved as a stable anode. However, the potential that was reached could be not low enough to promote bioH_2 production at the cathode tubular membrane. In order to reach lower potentials, N_2 flow was replaced by a small vacuum of about 80 kPa in the membrane (Figure 3A). Figure 3B reports the kinetic of the potential and current measured between the two electrodes when the vacuum was applied and stopped. Results indicated that a potential as low as -323 mV was reached and a negative current was continuously measured, varying from -0.53 µA/cm² (at the beginning of the experiment) to -1.1 µA/cm² (at the end of the experiment). In these conditions, a functional cathode was thus established, offering, among the series of experiments, the most compatible redox environment for hydrogen producers. When the vacuum was stopped, some oxygen probably entered into the membrane, resulting in a current that gradually increased (from 3h to 18h of the kinetic). The potential of the system was then gradually increasing up to -300 mV, which still remains more negative than during the previous experiment when N_2 was stopped (-100 mV) in the second design of the bioreactor design. One can assume that the risk of oxygen contamination is lower with the use of vacuum than with N_2 as the carrier gas. At the final stage of the experiment, the lowest potential was finally recovered when the vacuum was applied again (Figure 3B).

In conclusion, applying a vacuum in the conductive tubular membrane allowed reaching the lowest possible equilibrium potential of -323 mV vs SHE in the manure when this electrode was connected to a larger graphite felt while the two first designs did not show a low potential that can be maintained. Different cyclic voltammetry measurements were performed on the tubular membrane, allowing to observe oxygen contamination when vacuum, air or N_2 were used, when vacuum was stopped or when no gas flow was used in the membrane (figure 4B). Results indicated that the reduction curve tended to higher potentials in presence of air or in absence of any gas flow in the tubular membrane that did not passed below -200 mV vs SHE. However, lowest reduction curve potentials were observed with a N_2 flow, in the presence of a vacuum and even when the vacuum was stopped.

In the third design of the bioreactor, the tubular membrane became systematically the cathode, and the graphite felt the anode, which should correspond to different electrochemical reactions on these electrodes. To verify this electrode differentiation, cyclic voltammetry measurements were done with the graphite felt and the tubular membrane as individual electrodes. Results indicated dramatic differences between them. With the graphite felt, an anodic wave was

observed (Figure 4A, curve a), starting from a potential slightly more negative than -300 mV while such anodic wave was not observed at the tubular membrane (Figure 4A, curve b). The current at the tubular membrane was negative with a potential below -300 mV, which is consistent with the low cathodic current measured in short-circuit (Figure 3B). Such low current flow should not affect dramatically the bioH_2 production by direct reduction of proton but could induce favorable electrofermentation. This potential role of electrofermentation for bioH_2 production was further evaluated by combining electrochemical measurements and gas analyses (see next section).

3.2. Online monitoring of gas production during the DF-SCE experiment

In order to evaluate the environment generated in the third design of the bioreactor, i.e. with the optimal setup and electrode implementation, and to verify its capability to promote bioH_2 production, the bioreactor was connected to an online Micro Gas chromatography analyzer, both at the headspace and at the tubular cathode. The bioreactor was also connected to a potentiostat in order to evaluate the potential and current state that the system could naturally reach in these conditions. Since the reactor was inoculated with manure coming from a methanizer, it was assumed that the whole system was able to naturally produced CH_4, whereas bioH_2 is usually not detected in the atmosphere of such environment (Lebranchu et al. 2019). However, there are effective methods for favoring bioH_2 (from dark fermentation) over CH_4 (anaerobic digestion) and one of the most efficient consists in applying heat treatment to the bioreactor (Castelló et al. 2020).

Figure 5 shows electrochemical analysis at the beginning of the process with the whole medium, i.e. manure collected from the methanizer (Figure 5A) and with the same medium heat treated twice at 121 °C for 20 min (Figure 5B). When the medium was not heat treated, the potential of the whole system was stable and reached -277 mV with a stable current density established at -0.086 µA/cm² (Figure 5A). Such low potential was not observed when the inoculation of the bioreactor occurred after a heat treatment of the manure. In these experimental conditions the potential of the system reached only -42 mV with a stable current at -0.098 µA/cm² (Figure 5B). Results indicated that the heat treatment was not favorable to establish the bioelectrochemical system and did not allow reaching the low potential that was targeted (-300 mV). Moreover, gas analysis indicated that no bioH_2 was produced in the reactor with heat treated manure (Figure A, see annex). In addition, current measurements showed that the electrochemical system was slightly altered after each gas analysis, resulting in a brief increase in the cathode current value (this was observed for both reactors).

Electrochemical data measurements and the gas analysis, either in the tubular membrane and in the headspace of the reactor were carried out using this configuration of the process (Figure 6). In this experiment, the resilience and stability of the bioreactor were evaluated during the first 4 steps of the process. In particular, the two first stages described the beginning of the experiment and its stabilization before and after heat treatment respectively. The two last stages were carried out to illustrate the stability and resilience of the microbial based electrochemistry phenomenon after disconnection and re-connection of electrodes respectively, as shown by gas analysis and electrochemical measurements. In addition, to avoid the negative influence of gas analysis on electrochemical data, current and potential values were always collected just before gas samplings and analysis.

At the beginning of the experiment, CH_4 was detected in the tubular membrane in low amount, around 0.028%mol, then in higher quantity after 110 hours of culture with a maximum at 0.20 %mol (Figure 6B). BioH_2 was also detected through the membrane, and started to increase after 110 hours of culture and remained stable at 0.20%mol during this experiment. In the headspace of the bioreactor (Figure 6C), CH_4 production was also measured, from 0.15%mol at the beginning of the experiment, up to 0.22%mol after 100 hours of culture, while bioH_2 production reached a maximum value of 0.22%mol after 44 hours of culture before to remain stable at 0.18%mol. Before heat treatment, CH_4 production in the headspace of the bioreactor was always higher than bioH_2 production compared to the tubular membrane, showing that biomethanation was very active in these conditions.

After heat treatment, CH_4 decreased in the headspace of reactor, starting from 0.39 % mol to 0.07 %mol after 230 hours of the culture (Figure 6C). Production of this gas also decreased in the tubular membrane, going from 0.14 %mol, down to 0.05 %mol (Figure 6B). For both the headspace and the membrane, CH_4 was completely abolished after 338 hours of culture for the membrane and 374 hours in the headspace of reactor. Conversely, bioH_2 production increased in both compartments, with a higher amount detected through the membrane than in the headspace. In fact, the maximum amount of H_2 detected in the membrane was 0.37 %mol after 284 h instead of 0.26 %mol at the same time in the headspace of the reactor. Then, the gas production decreased and stabilized at 0.34 %mol through the tubular membrane and at 0.24 %mol in the headspace of the bioreactor respectively. In parallel, electrochemical measurements showed a temporary drop in potential of the system that reached -429 mV, at the lowest and a maximum of current density at -0.81 $\mu A/cm^2$, which was highly unexpected, but suggesting that the medium evolved to a very reductive environment, probably due to the excess

of hydrogen produced in the media. The electrode potential stabilized at values closed to -300 mV with a current density at -0.11 µA/cm² until 344 h. An increase in current density to -0.66 µA/cm², was then observed at 360 hours at the same potential. In fact, due to the vacuum created in the membrane, bioH_2 was directly collected when produced. The P_{H2} is one of the critical parameters in DF for bioH_2 production and high values of H_2 pressure could inhibit its own production during DF (Chung 1976; Kim et al. 2006; Jung et al. 2011; Zhou et al. 2017).

On the basis of these results, the hypothesis that the current generated by the bioreactor could be responsible for the direct bioH_2 production or was the consequence of the implementation of a favorable environment at the vicinity of the membrane that promoted DF microorganism species, had to be investigated. Moscoviz and al., proposed a coefficient based on Faradic yield, called electro-fermentation efficiency η_{EF} (Moscoviz and al., 2016). In this study, the index value of our system was 0.0018 at the tubular membrane, indicating that electron flow measured in the electrochemical system could not be directly linked to the H_2 production. Therefore, the hypothesis that the microenvironment created next to the electrodes could promote bioH_2 production by microorganisms was privileged. In fact, bioH_2 can be naturally produced by electro-active microorganisms that are able to give or receive electrons to or from the environment, and particularly these capabilities can help fermentative microorganisms by oxidizing products from fermentation into CO_2 and protons (Bhagchandanii et al. 2020; Schievano et al. 2016). Thus, specific environmental conditions created by anode and cathode may impact the redox potential, near the electrodes, that could promote bioH_2 production by microorganisms (Moscoviz et al. 2016).

In order to observe if the SCE implementation on the bioreactor could have a direct influence on gas production, electrodes were disconnected from 366 h to 471h. CH_4 was not detected and H_2 slightly decrease from 0.33 and 0.23 %mol to 0.29 and 0.19 %mol through the membrane and in the headspace, respectively. After electrodes reconnection at 471h, the electrochemical properties were restored, gas analyses indicated that bioH_2 production did not increase through the membrane and stays around 0.31 %mol whereas CH_4 remained undetectable. In the headspace of the bioreactor, the H_2 production increased slightly, reaching 0.21 %mol, suggesting a minor contribution of SCE on bioH_2 production. Concerning electrochemical measurements, the potential stabilized at -264 mV with a current density of -0.78 A/m². These values were consistent with the data measured at the beginning of the experiment. A direct link between electron flow and hydrogen production was not observed, supporting the idea that the

bioH_2 production was mainly due to DF microorganisms, and electrofermentation in a lesser extent.

3.3. Microbial analysis

To verify that hydrogen production was the result of a microbial activity and especially a microbial specialization in the bioreactor during the process kinetic, either in the whole medium or in the vicinity of electrodes, analysis of the microbial ecology was carried out. In details, microbial analyses were performed on the media; i.e. manure, at the beginning of the experiment, before heat treatment and at the end of the process, after heat treatment. Biofilm presents on the surface of tubular membrane (cathode) and graphite felt (anode) were also analyzed in order to see the impact of the bioreactor configuration on the implementation of microbial population on electrodes before and after heat treatment.

The figure 7 shows the microbial diversity found in medium samples and biofilm from anode and cathode before heat treatment and after heat treatment. The results from figure 7A did not showed any significant difference in richness (ASV number) between cathode, the medium and anode, at the stating of the experiment, and before and after heat treatment. Onn the other hand, Shannon index (figure 7B) presented a significative difference, after heat treatment, between the cathode biofilm that hosted more diversity than the anode and medium. The PCoA of the microbial communities confirmed this result (figure 8). In fact, the structure of bacterial communities is strongly affected by the thermic treatment (according to axis 1, which explained more than 67% of the variability). In addition, after heat treatment, the structure differed between the group's cathode/ medium and the anode.

In order to understand the impact of the heat treatment on the microbial communities, the microbial composition of samples from the media at the beginning and at the end of the experiment, as well as biofilms on the anode and the cathode, have been analyzed. The main populations found and presented at the class taxonomic level, is showed on the figure 9. Six main classes were observed: *Bacteroidia, Cloacimonadia Clostridia, Gammaproteobacteria*, *Limochordia* and *Spirochaetia*. There are no obvious differences in microbial community compositions between the beginning of the experiment, and before the heat treatment, either at class o taxonomical level. However, after the heat treatment, we observed a change in the communities in the three environments, i.e. anode, cathode and medium, with a drastic decrease in Cloacimonadales, for example, and an increase in the relative abundance of

Pseudomonadales. Interestingly, the anode showed higher relative abundances of the Clostridia class after heating treatment.

To confirm this result, a heatmap have been done with abundancy values in order to observe significant differences between population at the taxonomic class level on samples taken from manure after heat treatment (figure 10). At the lower taxonomic level and only after heat treatmentthe relative abundance of minority classes did not present any difference, excepted for *Cloacimonadia* that were found in higher quantity in the mediaat the end of the process. However, the anode displayed a different pattern compared to the cathode and the medium, with an under-representation of *Gammaproteobacteria* and *Bacteroidia.*. Moreover, an increase in relative abundance of *Clostridia* and *Bacilli* Class was shown at the anode with 56.5 and 7.2 respectively while the cathode and the medium showed a lower relative abundances of 25 and 4 respectively.In fact, *Gammaproteobacteria* and *Bacteroidia* are able to produce bioH_2 as well as *Clostridia* and *Bacilli* for some species, *Gammaproteobacteria* are also known to be electroactives bacteria such as *Shewanella* sp.

Moreover, because of their electroactive capabilities, species from those main classes found at the cathode may be electrotrophic, resulting in additional bioH_2 production. Those microorganisms were less present on the graphite felt that was composed in majority with *Clostridia*, sporulating species involved in the degradation of lignocellulosic materials, and in the production of acetate and bioH_2 The relative high abundancy of *Clostridia* on the graphite felt may suggest that those species, mainly exoelectrogenic, could be involved in the electrons transfer from the anode to the cathode (Ottoni et al. 2021; Wirth et al. 2012; Logan et al. 2019). Thus, it was supposed that combining activities of specialized microorganisms on both electrodes in such SCE-DF bioprocess may favor substrate oxidation, enhancing bioH_2 production. Some other electroactive microorganisms belonging to *Geobacter*, or *Clostridium* species, that are part of the *Gammaproteobacteria* or *Clostridia* class respectively, are usually found in those systems using agricultural wastes, have the capacity to oxidize acids such as VFAs or more complex subtract such as cellulose (Ndayisenga et al. 2021; Logan et al. 2019). It has to be noticed that some species from those phyla may not be electroactives too. Besides, it was expected that electroactive and non-electroactive microbes were present in biofilms, interacting together in symbiosis, as revealed by metagenomic analyses. However, the role of the latter remained unknown or at least could not be revealed in this study, and further experimentations are needed to characterize them and to confirm the importance of electroactives bacteria in this dual SCE-DF bioprocess for bioH_2 production.

4. Conclusion

In this study, a bioH_2 production process combining short-circuited electrodes with dark fermentation was evaluated. Results indicated that potential as low as -320 mV vs SHE could be reached with manure when electrodes made with a graphite felt and a tubular membrane were short–circuited resulting in a specialization in a functional anode and cathode, respectively. In these experimental conditions and after heat treatment, a negative current was observed at the tubular membrane surface, resulting in bioH_2 production higher in the membrane than in the headspace of the bioreactor. Such electrode specialization was confirmed by microbial ecology analyses and cyclic voltammetry measurements. Based on this pioneering work, additional studies are needed for further characterization of the process and improvement of bioH_2 production.

Aknowledgements

The research was supported by the LUE program UHLYS of the University of Lorraine, FRCR project 3BR, and ERDF project TALISMAN2. The authors wish to thank Benjamin Rivard and Adrienne Mangin of the experimental farm “La Bouzule” of University of Lorraine, Nancy, France, and Vincent Bourot of “Methanason, Einville-au-Jard, France.

References

Andersen, K. S., Kirkegaard, R. H., Karst, S. M., & Albertsen, M. 2018. Ampvis2: an R package to analyse and visualise 16S rRNA amplicon data. BioRxiv, 299537.

Barca, Cristian, David Ranava, Marielle Bauzan, Jean-Henry Ferrasse, Marie-Thérèse Giudici-Orticoni, et Audrey Soric. 2016. « Fermentative Hydrogen Production in an Up-Flow Anaerobic Biofilm Reactor Inoculated with a Co-Culture of *Clostridium Acetobutylicum* and *Desulfovibrio Vulgaris* ». Bioresource Technology 221: 526-33. https://doi.org/10.1016/j.biortech.2016.09.072.

Andersen, K. S., Kirkegaard, R. H., Karst, S. M., & Albertsen, M. 2018. Ampvis2: an R package to analyse and visualise 16S rRNA amplicon data. BioRxiv, 299537.

Bokulich, N. A., Subramanian, S., Faith, J. J., Gevers, D., Gordon, J. I., Knight, R., ... & Caporaso, J. G. 2013. Quality-filtering vastly improves diversity estimates from Illumina amplicon sequencing. *Nature methods*, *10*(1), 57-59.

Bhagchandanii, Drishti Dinesh, Rishi Pramod Babu, Jayesh M. Sonawane, Namita Khanna, Soumya Pandit, Dipak A. Jadhav, Santimoy Khilari, et Ram Prasad. 2020. « A Comprehensive Understanding of Electro ». Fermentation 6 (3): 92. https://doi.org/10.3390/fermentation6030092.

Camacho, C., Coulouris, G., Avagyan, V., Ma, N., Papadopoulos, J., Bealer, K., & Madden, T. L. 2009. BLAST+: architecture and applications. BMC bioinformatics, 10, 1-9.

Castelló, Elena, Antonio Djalma Nunes Ferraz-Junior, Cristiane Andreani, Melida Del Pilar Anzola-Rojas, Liliana Borzacconi, Germán Buitrón, Julián Carrillo-Reyes, et al. 2020. « Stability Problems in the Hydrogen Production by Dark Fermentation: Possible Causes and Solutions ». Renewable and Sustainable Energy Reviews 119: 109602. https://doi.org/10.1016/j.rser.2019.109602.

Cheng, S., et B. E. Logan. 2007. « Sustainable and Efficient Biohydrogen Production via Electrohydrogenesis ». Proceedings of the National Academy of Sciences 104 (47): 18871-73. https://doi.org/10.1073/pnas.0706379104.

Chung, K T. 1976. « Inhibitory Effects of H2 on Growth of *Clostridium Cellobioparum*. » Applied and Environmental Microbiology 31 (3): 342-48. https://doi.org/10.1128/AEM.31.3.342-348.1976.

Erable, B, L. Etcheverry, A. Bergel, 2011. From microbial fuel cell (MFC) to microbial electrochemical snorkel (MES): maximizing chemical oxygen demand (COD) removal from wastewater., Biofouling. 27: 319–326.

Escudié, F., Auer, L., Bernard, M., Mariadassou, M., Cauquil, L., Vidal, K., ... & Pascal, G. 2018. FROGS: find, rapidly, OTUs with galaxy solution. *Bioinformatics*, *34*(8), 1287-1294.

Fan, Qingwen, Xiaojing Fan, Peng Fu, Yongmei Sun, Yan Li, Siling Long, Tianyang Guo, Liang Zheng, Kai Yang, et Dongliang Hua. 2022. « Microbial Community Evolution, Interaction, and Functional Genes Prediction during Anaerobic Digestion in the Presence of Refractory Organics ». Journal of Environmental Chemical Engineering 10 (3): 107789. https://doi.org/10.1016/j.jece.2022.107789.

Ghimire, Anish, Luigi Frunzo, Francesco Pirozzi, Eric Trably, Renaud Escudie, Piet N.L. Lens, et Giovanni Esposito. 2015. « A Review on Dark Fermentative Biohydrogen Production from Organic Biomass: Process Parameters and Use of by-Products ». Applied Energy 144: 73-95. https://doi.org/10.1016/j.apenergy.2015.01.045.

Guo, Kun, Antonin Prévoteau, et Korneel Rabaey. 2017. « A Novel Tubular Microbial Electrolysis Cell for High Rate Hydrogen Production ». Journal of Power Sources 356 : 484-90. https://doi.org/10.1016/j.jpowsour.2017.03.029.

Guo, Xin Mei, Eric Trably, Eric Latrille, Hélène Carrère, et Jean-Philippe Steyer. 2010. « Hydrogen Production from Agricultural Waste by Dark Fermentation: A Review ». International Journal of Hydrogen Energy 35 (19): 10660-73. https://doi.org/10.1016/j.ijhydene.2010.03.008.

Hoareau, Morgane, Luc Etcheverry, Olivier Chapleur, Chrystelle Bureau, Cédric Midoux, Benjamin Erable, et Alain Bergel. 2023. « The Electrochemical Microbial Tree: A New Concept for Wastewater Treatment ». Chemical Engineering Journal 454 : 140295. https://doi.org/10.1016/j.cej.2022.140295.

Hubenova, Y., Chorbadzhiyska, E., Kostov, K.L., Mitov, M. 2023. Efficient gold recovery by microbial electrochemical technologies, Bioelectrochemistry. 149: 108311. doi:10.1016/j.bioelechem.2022.108311 CO - BIOEFK.

Jeremiasse, Adriaan W., Hubertus V.M. Hamelers, Michel Saakes, et Cees J.N. Buisman. 2010. « Ni Foam Cathode Enables High Volumetric H2 Production in a Microbial Electrolysis Cell ». International Journal of Hydrogen Energy 35 (23): 12716-23. https://doi.org/10.1016/j.ijhydene.2010.08.131.

Jumas-Bilak, Estelle, et Hélène Marchandin. 2014. « The Phylum *Synergistetes* ». In The Prokaryotes, edited by Eugene Rosenberg, Edward F. DeLong, Stephen Lory, Erko

Stackebrandt, and Fabiano Thompson, 931-54. Berlin, Heidelberg: Springer Berlin Heidelberg. https://doi.org/10.1007/978-3-642-38954-2_384.

Jung, Kyung-Won, Dong-Hoon Kim, Sang-Hyoun Kim, et Hang-Sik Shin. 2011. « Bioreactor Design for Continuous Dark Fermentative Hydrogen Production ». Bioresource Technology 102 (18): 8612-20. https://doi.org/10.1016/j.biortech.2011.03.056.

Katuri, Krishna P., Craig M. Werner, Rodrigo J. Jimenez-Sandoval, Wei Chen, Sungil Jeon, Bruce E. Logan, Zhiping Lai, Gary L. Amy, et Pascal E. Saikaly. 2014. « A Novel Anaerobic Electrochemical Membrane Bioreactor (AnEMBR) with Conductive Hollow-Fiber Membrane for Treatment of Low-Organic Strength Solutions ». Environmental Science & Technology 48 (21): 12833-41. https://doi.org/10.1021/es504392n.

Kim, D, S Han, S Kim, et H Shin. 2006. « Effect of Gas Sparging on Continuous Fermentative Hydrogen Production ». International Journal of Hydrogen Energy 31 (15): 2158-69. https://doi.org/10.1016/j.ijhydene.2006.02.012.

Kumar, G. Gnana, V.G. Sathiya Sarathi, et Kee Suk Nahm. 2013. « Recent Advances and Challenges in the Anode Architecture and Their Modifications for the Applications of Microbial Fuel Cells ». Biosensors and Bioelectronics 43: 461-75. https://doi.org/10.1016/j.bios.2012.12.048.

Lalaurette, Elodie, Shivegowda Thammannagowda, Ali Mohagheghi, Pin-Ching Maness, et Bruce E. Logan. 2009. « Hydrogen Production from Cellulose in a Two-Stage Process Combining Fermentation and Electrohydrogenesis ». International Journal of Hydrogen Energy 34 (15): 6201-10. https://doi.org/10.1016/j.ijhydene.2009.05.112.

L. Bräuer, Suzanna, Nathan Basiliko, Henri M. P. Siljanen, et Stephen H. Zinder. 2020. « Methanogenic Archaea in Peatlands ». FEMS Microbiology Letters 367 (20): fnaa172. https://doi.org/10.1093/femsle/fnaa172.

Lebranchu, Aline, Fabrice Blanchard, Michel Fick, Stéphane Pacaud, Eric Olmos, et Stéphane Delaunay. 2019. « Pilot-Scale Biomethanation of Cattle Manure Using Dense Membranes ». Bioresource Technology 284: 430-36. https://doi.org/10.1016/j.biortech.2019.03.140.

Lee, Kuo-Shing, Tzu-Shan Tseng, Yen-Wen Liu, et Yi-Dai Hsiao. 2012. « Enhancing the Performance of Dark Fermentative Hydrogen Production Using a Reduced Pressure Fermentation Strategy ». International Journal of Hydrogen Energy 37 (20): 15556-62. https://doi.org/10.1016/j.ijhydene.2012.04.039.

Liu, Wenzong, Shihching Huang, Aijuan Zhou, Guangyu Zhou, Nanqi Ren, Aijie Wang, et Guoqiang Zhuang. 2012. « Hydrogen Generation in Microbial Electrolysis Cell Feeding with Fermentation Liquid of Waste Activated Sludge ». International Journal of Hydrogen Energy 37 (18): 13859-64. https://doi.org/10.1016/j.ijhydene.2012.04.090.

Logan, Bruce E., Ruggero Rossi, Ala'a Ragab, et Pascal E. Saikaly. 2019. « Electroactive Microorganisms in Bioelectrochemical Systems ». Nature Reviews Microbiology 17 (5): 307-19. https://doi.org/10.1038/s41579-019-0173-x.

McMurdie, P. J., & Holmes, S. 2013. phyloseq: an R package for reproducible interactive analysis and graphics of microbiome census data. *PloS one*, *8*(4), e61217.Mahé, F., Czech, L., Stamatakis, A., Quince, C., de Vargas, C., Dunthorn, M., & Rognes, T. 2022. Swarm v3: towards tera-scale amplicon clustering. *Bioinformatics*, *38*(1), 267-269

Mitov, Mario, Ivo Bardarov, Elitsa Chorbadzhiyska, Krassimir L. Kostov, et Yolina Hubenova. 2021. « First evidence for applicability of the microbial electrochemical snorkel for metal recovery ». Electrochemistry Communications 122: 106889. https://doi.org/10.1016/j.elecom.2020.106889.

M. Mitov, M., Chorbadzhiyska, E., Bardarov, I., Kostov, K.L, Hubenova, Y. 2022. Silver recovery by microbial electrochemical snorkel and microbial fuel cell, Electrochim. Acta. 408 : 139941.

Mizuno, Osamu, Richard Dinsdale, Freda R Hawkes, Dennis L Hawkes, et Tatsuya Noike. 2000. « Enhancement of Hydrogen Production from Glucose by Nitrogen Gas Sparging ». Bioresource Technology, 7.

Moreno, R., A. Escapa, J. Cara, B. Carracedo, et X. Gómez. 2015. « A Two-Stage Process for Hydrogen Production from Cheese Whey: Integration of Dark Fermentation and Biocatalyzed Electrolysis ». International Journal of Hydrogen Energy 40 (1): 168-75. https://doi.org/10.1016/j.ijhydene.2014.10.120.

Morsy, Fatthy Mohamed. 2017. « Synergistic Dark and Photo-Fermentation Continuous System for Hydrogen Production from Molasses by Clostridium Acetobutylicum ATCC 824 and Rhodobacter Capsulatus DSM 1710 ». Journal of Photochemistry and Photobiology B: Biology 169: 1-6. https://doi.org/10.1016/j.jphotobiol.2017.02.011.

Mosca, Lorena, Jose Antonio Medrano Jimenez, Solomon Assefa Wassie, Fausto Gallucci, Emma Palo, Michele Colozzi, Stefania Taraschi, et Giulio Galdieri. 2020. « Process Design for Green Hydrogen Production ». International Journal of Hydrogen Energy 45 (12): 7266-77. https://doi.org/10.1016/j.ijhydene.2019.08.206.

Moscoviz, Roman, Javiera Toledo-Alarcón, Eric Trably, et Nicolas Bernet. 2016. « Electro-Fermentation: How To Drive Fermentation Using Electrochemical Systems ». Trends in Biotechnology 34 (11): 856-65. https://doi.org/10.1016/j.tibtech.2016.04.009.

Ndayisenga, Fabrice, Zhisheng Yu, Jianzhong Zheng, Bobo Wang, Hongxia Liang, Irfan Ali Phulpoto, Telesphore Habiyakare, et Dandan Zhou. 2021. « Microbial Electrohydrogenesis Cell and Dark Fermentation Integrated System Enhances Biohydrogen Production from Lignocellulosic Agricultural Wastes: Substrate Pretreatment towards Optimization ». Renewable and Sustainable Energy Reviews 145 : 111078. https://doi.org/10.1016/j.rser.2021.111078.

Oh, Sang-Eun, Prabha Iyer, Mary Ann Bruns, et Bruce E. Logan. 2004. « Biological Hydrogen Production Using a Membrane Bioreactor ». Biotechnology and Bioengineering 87 (1): 119-27. https://doi.org/10.1002/bit.20127.

Ottoni, Júlia Ronzella, Suzan Prado Fernandes Bernal, Tiago Joelzer Marteres, Franciele Natividade Luiz, Viviane Piccin dos Santos, Ângelo Gabriel Mari, Juliana Gaio Somer, Valéria Maia de Oliveira, et Michel Rodrigo Zambrano Passarini. 2021. « Cultured and Uncultured Microbial Community Associated With Biogas Production ». Preprint. In Review. https://doi.org/10.21203/rs.3.rs-1107386/v1.

Patil, Sunil A., Falk Harnisch, Christin Koch, Thomas Hübschmann, Ingo Fetzer, Alessandro A. Carmona-Martínez, Susann Müller, et Uwe Schröder. 2011. « Electroactive Mixed Culture Derived Biofilms in Microbial Bioelectrochemical Systems: The Role of PH on Biofilm Formation, Performance and Composition ». Bioresource Technology 102 (20): 9683-90. https://doi.org/10.1016/j.biortech.2011.07.087.

Pruesse, E., Quast, C., Knittel, K., Fuchs, B. M., Ludwig, W., Peplies, J., & Glöckner, F. O. 2007. SILVA: a comprehensive online resource for quality checked and aligned ribosomal RNA sequence data compatible with ARB. *Nucleic acids research*, *35*(21), 7188-7196.

Reeve, Holly A., Philip A. Ash, HyunSeo Park, Ailun Huang, Michalis Posidias, Chloe Tomlinson, Oliver Lenz, et Kylie A. Vincent. 2017. « Enzymes as Modular Catalysts for Redox Half-Reactions in H2-Powered Chemical Synthesis: From Biology to Technology ». Biochemical Journal 474 (2): 215-30. https://doi.org/10.1042/BCJ20160513.

Renaudie, Marie, Christine Dumas, Stéphane Vuilleumier, et Barbara Ernst. 2021. « Biohydrogen Production in a Continuous Liquid/Gas Hollow Fiber Membrane Bioreactor: Efficient Retention of Hydrogen Producing Bacteria via Granule and

Biofilm Formation ». Bioresource Technology 319: 124203. https://doi.org/10.1016/j.biortech.2020.124203.

Rogińska, Joanna, Michel Perdicakis, Cédric Midoux, Théodore Bouchez, Christelle Despas, Liang Liu, Jiang-Hao Tian, et al. 2021. « Electrochemical Analysis of a Microbial Electrochemical Snorkel in Laboratory and Constructed Wetlands ». Bioelectrochemistry 142: 107895. https://doi.org/10.1016/j.bioelechem.2021.107895.

Rogińska, Joanna, Timothé Philippon, Morgane Hoareau, Frédéric P.A. Jorand, Frédéric Barrière, et Mathieu Etienne. 2023. « Challenges and Applications of Nitrate-Reducing Microbial Biocathodes ». Bioelectrochemistry 152: 108436. https://doi.org/10.1016/j.bioelechem.2023.108436.

Rognes, T., Scheffer, L., Greiff, V., & Sandve, G. K. 2022. CompAIRR: ultra-fast comparison of adaptive immune receptor repertoires by exact and approximate sequence matching. *Bioinformatics*, *38*(17), 4230-4232.

Rozendal, René A, Adriaan W Jeremiasse, Hubertus V M Hamelers, et Cees J N Buisman. 2008. « Hydrogen Production with a Microbial Biocathode », 6.

Saint-Amans, Sylvie, Laurence Girbal, Jose Andrade, Kerstin Ahrens, et Philippe Soucaille. 2001. « Regulation of Carbon and Electron Flow in Clostridium Butyricum VPI 3266 Grown on Glucose-Glycerol Mixtures ». Journal of Bacteriology 183 (5): 1748-54. https://doi.org/10.1128/JB.183.5.1748-1754.2001.

Schievano, Andrea, Tommy Pepé Sciarria, Karolien Vanbroekhoven, Heleen De Wever, Sebastià Puig, Stephen J. Andersen, Korneel Rabaey, et Deepak Pant. 2016. « Electro-Fermentation – Merging Electrochemistry with Fermentation in Industrial Applications ». Trends in Biotechnology 34 (11): 866-78. https://doi.org/10.1016/j.tibtech.2016.04.007.

Wang, Yun-Kun, Guo-Ping Sheng, Bing-Jing Shi, Wen-Wei Li, et Han-Qing Yu. 2013. « A Novel Electrochemical Membrane Bioreactor as a Potential Net Energy Producer for Sustainable Wastewater Treatment ». Scientific Reports 3 (1): 1864. https://doi.org/10.1038/srep01864.

Wang, Yun-Qi, Fang Zhang, Wei Zhang, Kun Dai, Hua-Jie Wang, Xue Li, et Raymond Jianxiong Zeng. 2018. « Hydrogen and Carbon Dioxide Mixed Culture Fermentation in a Hollow-Fiber Membrane Biofilm Reactor at 25 °C ». Bioresource Technology 249 : 659-65. https://doi.org/10.1016/j.biortech.2017.10.054.

Werner, Craig M., Krishna P. Katuri, Ananda Rao Hari, Wei Chen, Zhiping Lai, Bruce E. Logan, Gary L. Amy, et Pascal E. Saikaly. 2016. « Graphene-Coated Hollow Fiber

Membrane as the Cathode in Anaerobic Electrochemical Membrane Bioreactors – Effect of Configuration and Applied Voltage on Performance and Membrane Fouling ». Environmental Science & Technology 50 (8): 4439-47. https://doi.org/10.1021/acs.est.5b02833.

Wirth, Roland, Etelka Kovács, Gergely Maróti, Zoltán Bagi, Gábor Rákhely, et Kornél L Kovács. 2012. « Characterization of a Biogas-Producing Microbial Community by Short-Read next Generation DNA Sequencing ». Biotechnology for Biofuels 5 (1): 41. https://doi.org/10.1186/1754-6834-5-41.

Zagrodnik, R., et M. Łaniecki. 2017. « Hydrogen Production from Starch by Co-Culture of *Clostridium Acetobutylicum* and *Rhodobacter Sphaeroides* in One Step Hybrid Dark- and Photofermentation in Repeated Fed-Batch Reactor ». Bioresource Technology 224 : 298-306. https://doi.org/10.1016/j.biortech.2016.10.060.

Zaybak, Zehra, John M. Pisciotta, Justin C. Tokash, et Bruce E. Logan. 2013. « Enhanced Start-up of Anaerobic Facultatively Autotrophic Biocathodes in Bioelectrochemical Systems ». Journal of Biotechnology 168 (4): 478-85. https://doi.org/10.1016/j.jbiotec.2013.10.001.

Zhou, Miaomiao, Jun Zhou, Ming Tan, Juan Du, Binghua Yan, Jonathan W.C. Wong, et Yang Zhang. 2017. « Enhanced Carboxylic Acids Production by Decreasing Hydrogen Partial Pressure during Acidogenic Fermentation of Glucose ». Bioresource Technology 245 (december): 44-51. https://doi.org/10.1016/j.biortech.2017.08.152.

Figure captions

Figure 1. (A) First design of the bioreactor and (B) Electrochemical evaluation of this reactor with utilization of air or N_2 as gas carriers in the tubular membrane. N_2 was flushed into the headspace at the experiment's outset to establish anaerobic conditions. The orange curve represents the potential, and the blue curve represents the current, recorded throughout the experiment.

Figure 2. (A) Second design of the bioreactor and (B) Electrochemical evaluation of this reactor with and without the utilization of N_2 as the tubular membrane's gas carrier. N_2 is introduced into the headspace at the experiment's outset to establish anaerobic conditions in the headspace. The orange curve represents the potential, and the blue curve represents the current recorded throughout the experiment.

Figure 3. (A) Third design of the bioreactor and (B) Electrochemical evaluation of this reactor under vacuum and without vacuum conditions. N_2 was introduced into the headspace at the experiment's outset to establish anaerobic conditions in the headspace. The orange curve represents the potential, and the blue curve represents the current recorded throughout the experiment.

Figure 4. Cyclic voltammetric measurements (A) on (a) the graphite felt and (b) the tubular membrane at the end of the experiment presented in Figure 3, with the third design of the bioreactor; and (B) carried out on the membrane in the first and third designs of the bioreactor (a) with vacuum, (b) after the vacuum was stopped, (c) without any gas carrier, (d) with N_2 as a gas carrier and (e) in presence of air as a gas carrier. All cyclic voltammetric measurements were done with a scan rate set at 1mV/s.

Figure 5. Potential (in orange curves) and current (in blue curves) measurements obtained from the setup comprising a tubular membrane short-circuited with a piece of graphite felt within the reactor. This was inoculated with (A) manure and (B) with manure after double heat treatment of 121 °C for 20 minutes.

Figure 6. Kinetic of electrochemical responses and gas analyses in the third design of the experiment. The experiment consisted in four consecutive phases: the "Starting" phase with untreated manure, the "After Heat Treatment" in which the bioreactor was heat treated twice at 121 °C for 20 min in order to inactivate methanogen species, the “Electrode disconnection” and “Electrode connection” in order to evaluate short-circuited electrodes on gas production. (A) electrochemical equilibrium potential and current analysis between the short-circuited tubular membrane and graphite felt throughout the entire experiment, (B) analysis of CH_4 and bioH_2 gas from the tubular membrane, (C) analysis of CH_4 and bioH_2 gas from the head of the reactor.

Figure 7. Microbial alpha diversity (diversity indices) between of microbial communities sampled in reactor at different time/treatments. A: The alpha diversity is presented as a measure of species richness (ASV number) and B: biodiversity index (Shannon index) Stars above the histograms indicate significant differences between treatments; *P < 0.05, **P <0.005 and ***P <0.001.

Figure 8: PcoA of microbial communities structure among different processes and time/treatments, based on weighted Unifrac Distance

Figure 9: Composition plot of microbial communities recovered from different area for each treatment at Class taxonomical level

Figure 10: Heatmap reporting on microbiota composition and relative abundances of bacterial at the class level among cathode, anode and medium for reactor 4 after heat treatment. Colors are scaled from highest (red) to lowest (blue) values within columns.

Figure A (supplementary material): Kinetic of electrochemical responses and gas analyses in the third design of the experiment with heatreated manure before inoculation. The experiment consisted in six consecutive phases - a: after two heat-treatment at 80 °C for 45 min, b: after two heat-treatment at 80 °C for 45 min, c: after one heat-treatment at 80°C for 2h30, d: after 2 heat-treatment at 121 °C for 20 min, e: after 2 heat-treatment at 121 °C for 20 min and f: after 3 heat-treatment at 121 °C for 1h. (A) electrochemical equilibrium potential and current analysis between the short-circuited tubular membrane and graphite felt throughout the entire experiment, (B) analysis of CH_4 and H_2 gas from the tubular membrane, (C) analysis of CH_4 and H_2 gas from the head of the reactor.

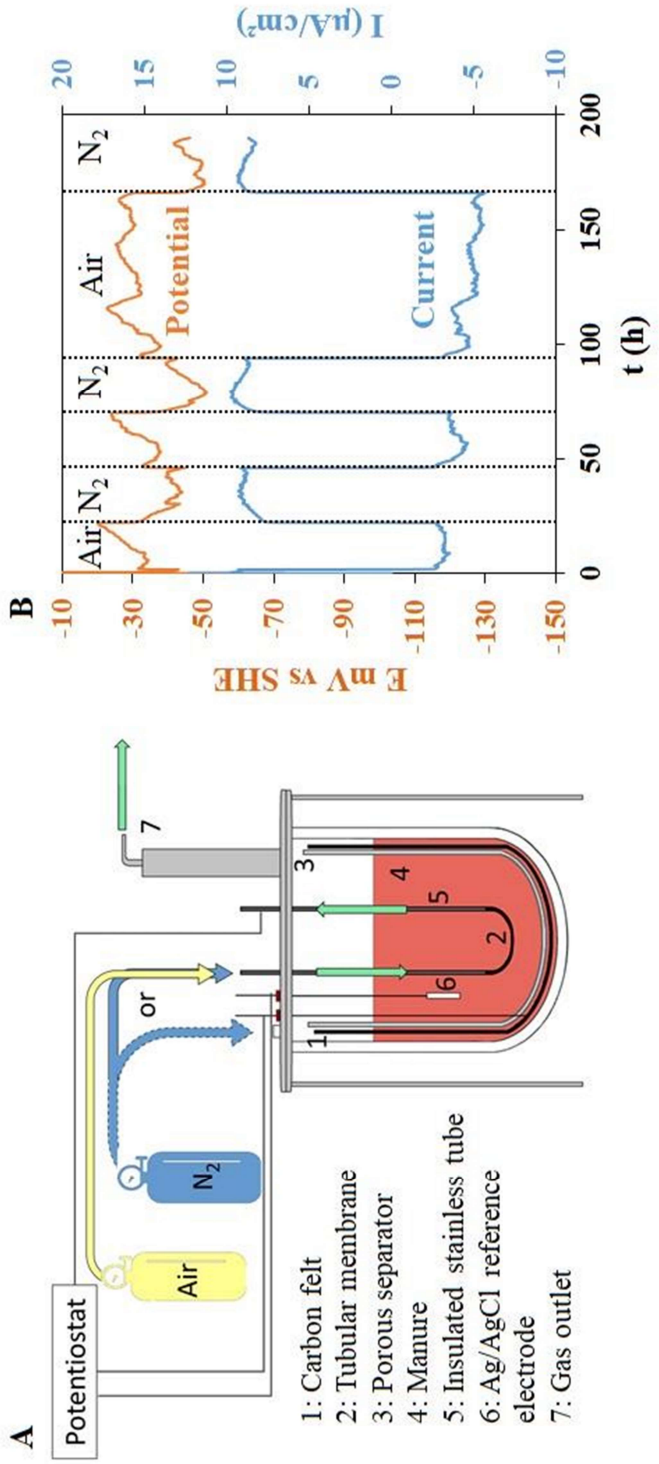
A
Potentiostat
Air
N2
or
1: Carbon felt
2: Tubular membrane
3: Porous separator
4: Manure
5: Insulated stainless tube
6: Ag/AgCl reference electrode
7: Gas outlet
B
E mV vs SHE
I (µA/cm²)
t (h)
Potential
Current
Air
N2
Air
N2
N2

Figure 1

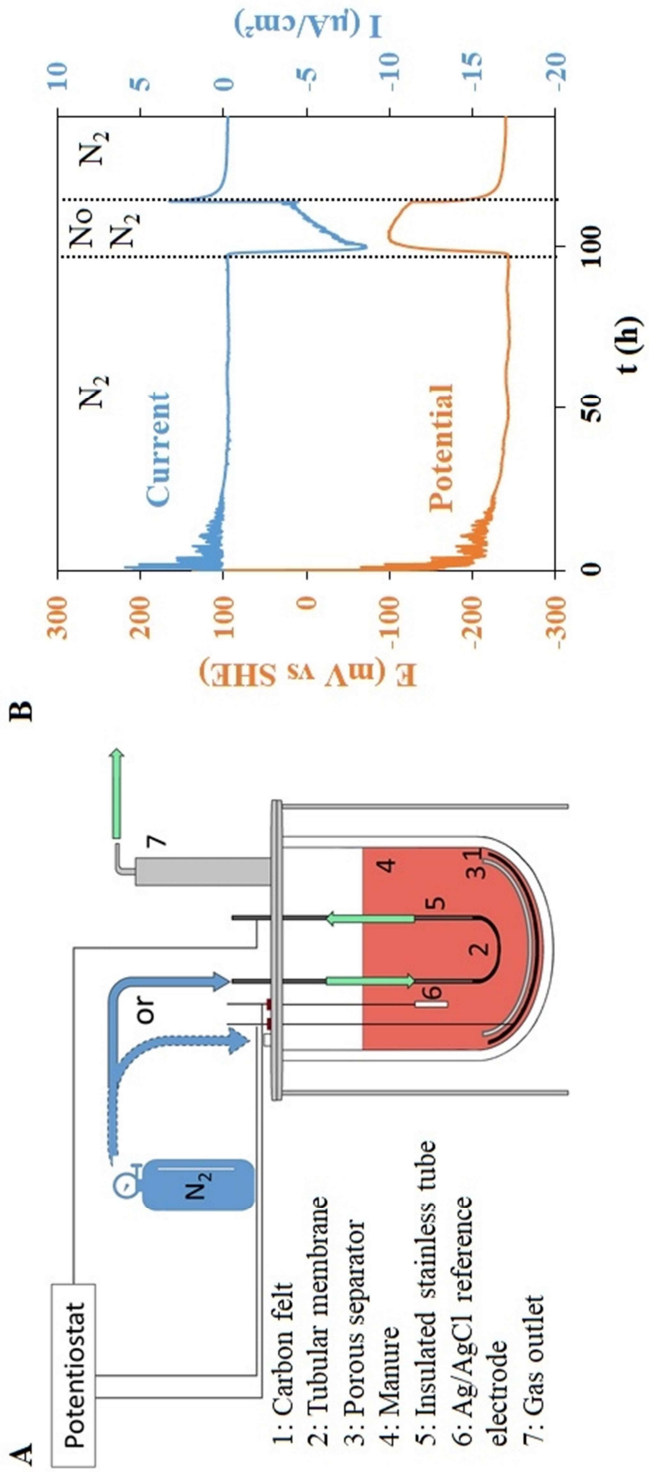
A
Potentiostat
N_2
or
1: Carbon felt
2: Tubular membrane
3: Porous separator
4: Manure
5: Insulated stainless tube
6: Ag/AgCl reference electrode
7: Gas outlet
B
E (mV vs SHE)
I (μA/cm²)
Current
Potential
N_2
No N_2
N_2
t (h)

Figure 2

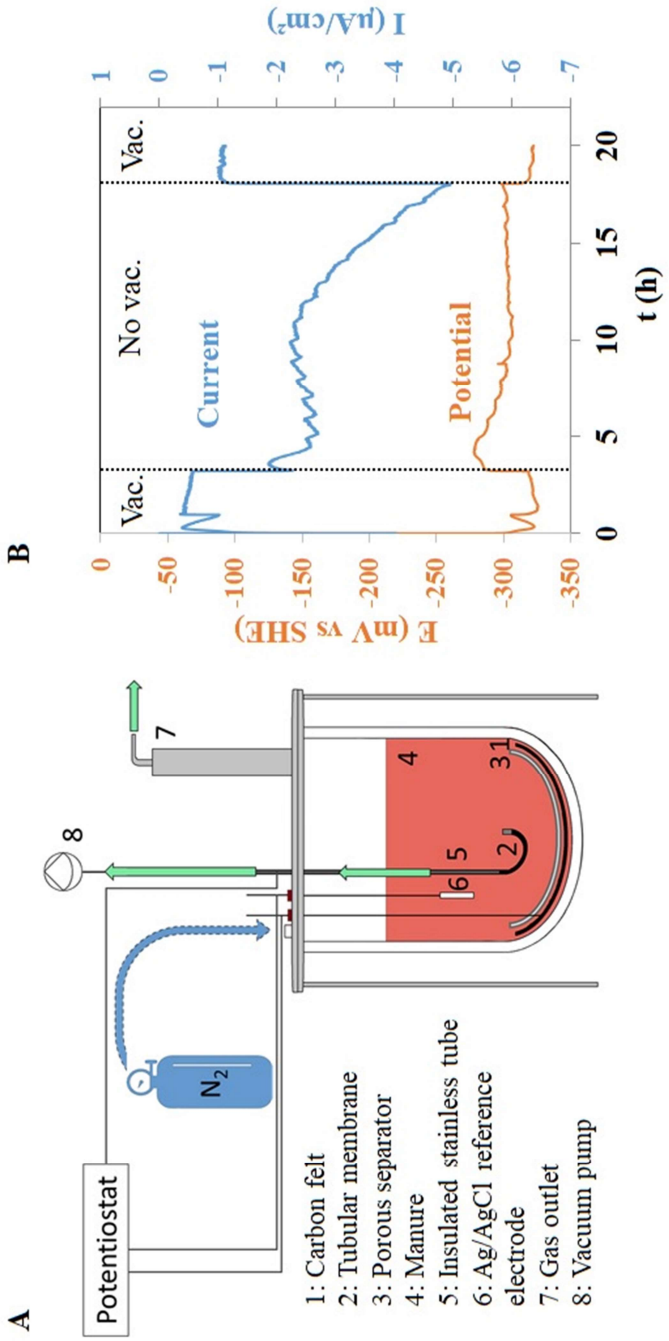
A
Potentiostat
N2
8
7
4
3
1
2
5
6
1: Carbon felt
2: Tubular membrane
3: Porous separator
4: Manure
5: Insulated stainless tube
6: Ag/AgCl reference electrode
7: Gas outlet
8: Vacuum pump
B
I (µA/cm²)
E (mV vs SHE)
Vac.
No vac.
Vac.
Current
Potential
t (h)

Figure 3

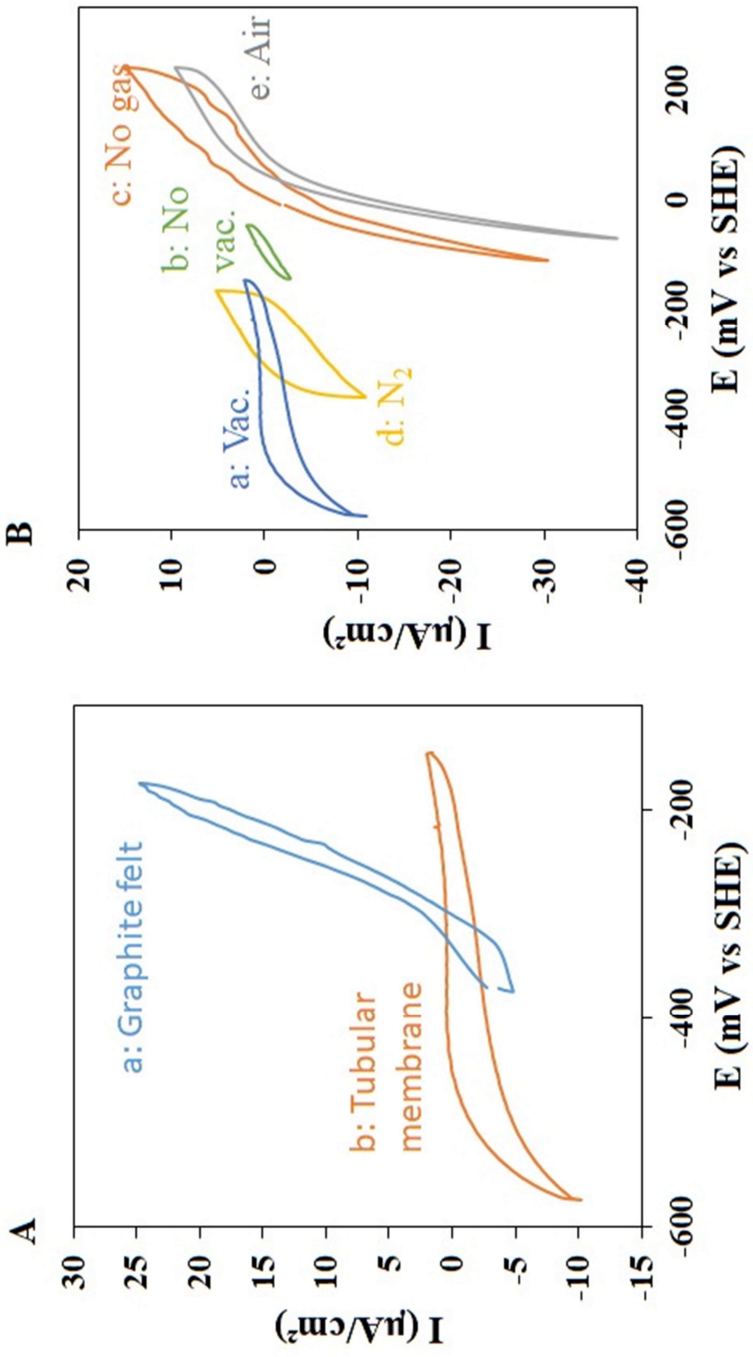
A
B
a: Graphite felt
b: Tubular membrane
a: Vac.
b: No vac.
c: No gas
d: N_2
e: Air
I (μA/cm²)
E (mV vs SHE)

Figure 4

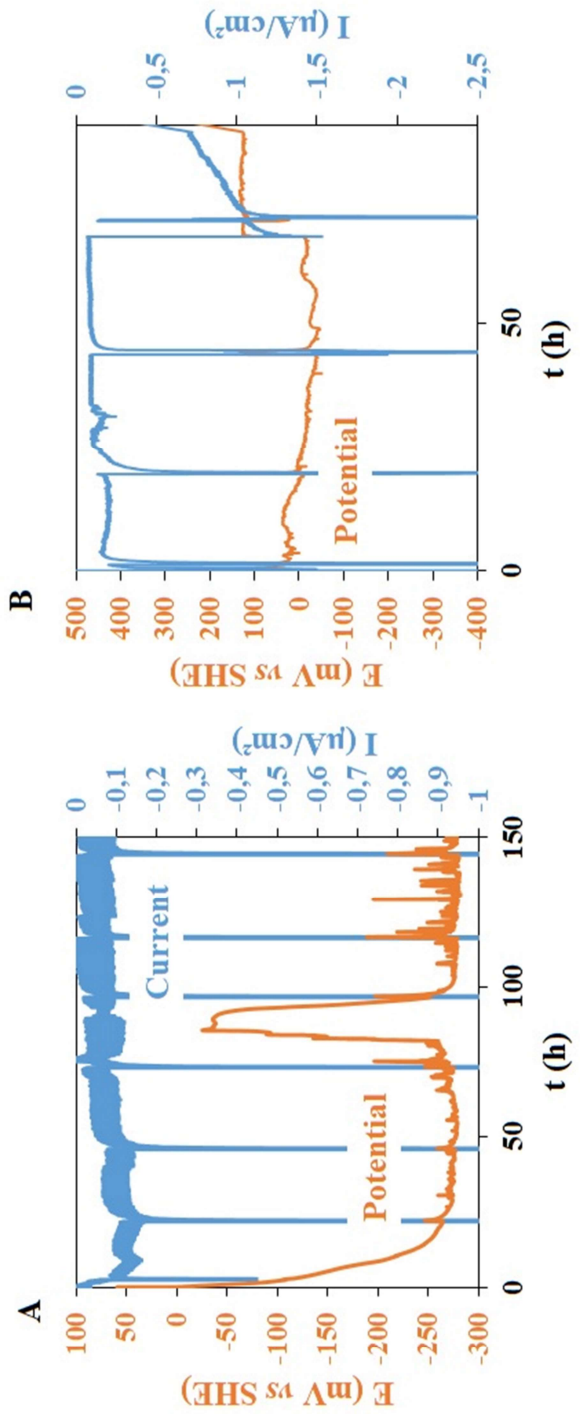

Figure 5

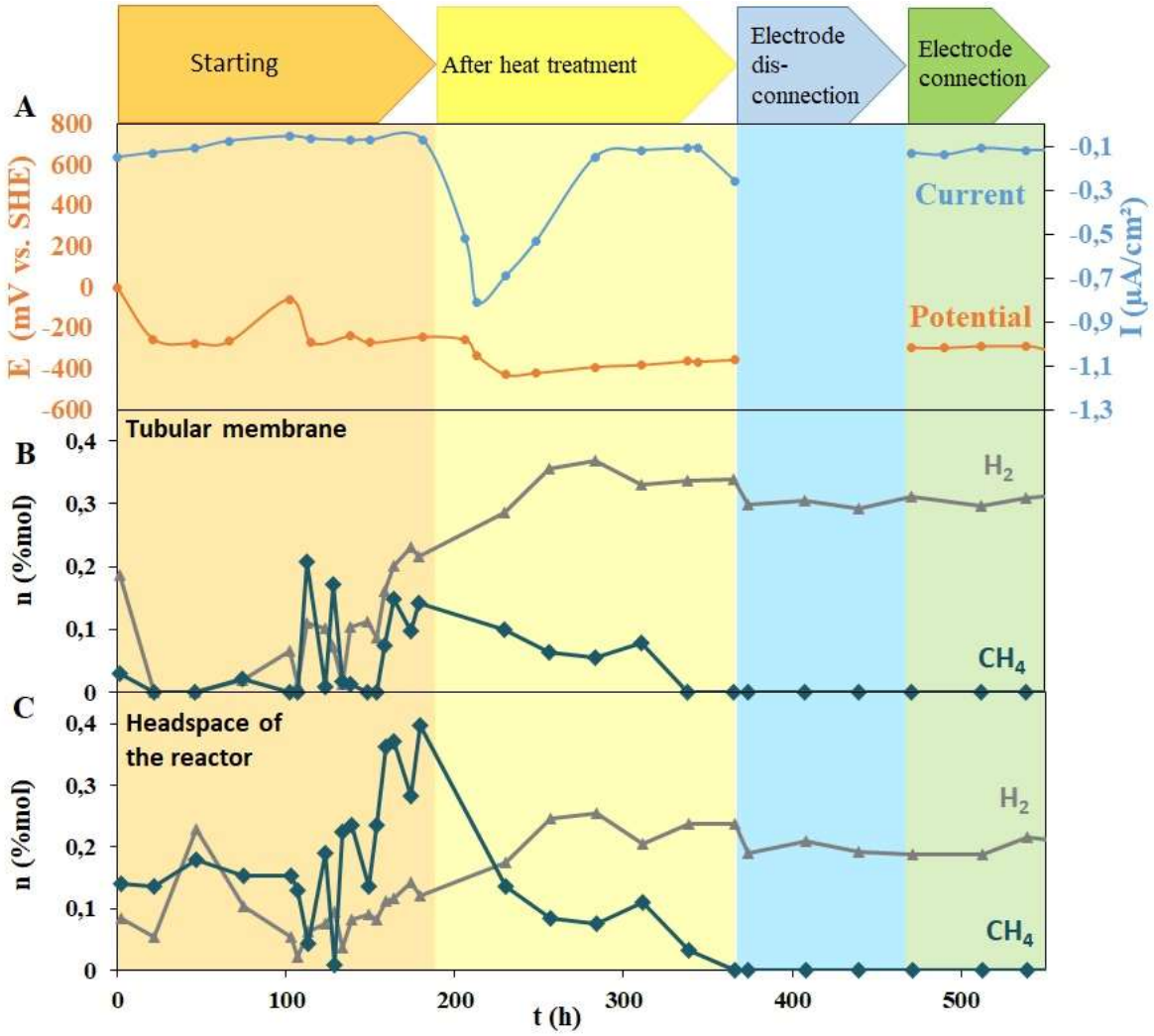

1

2

3 Figure 6

4

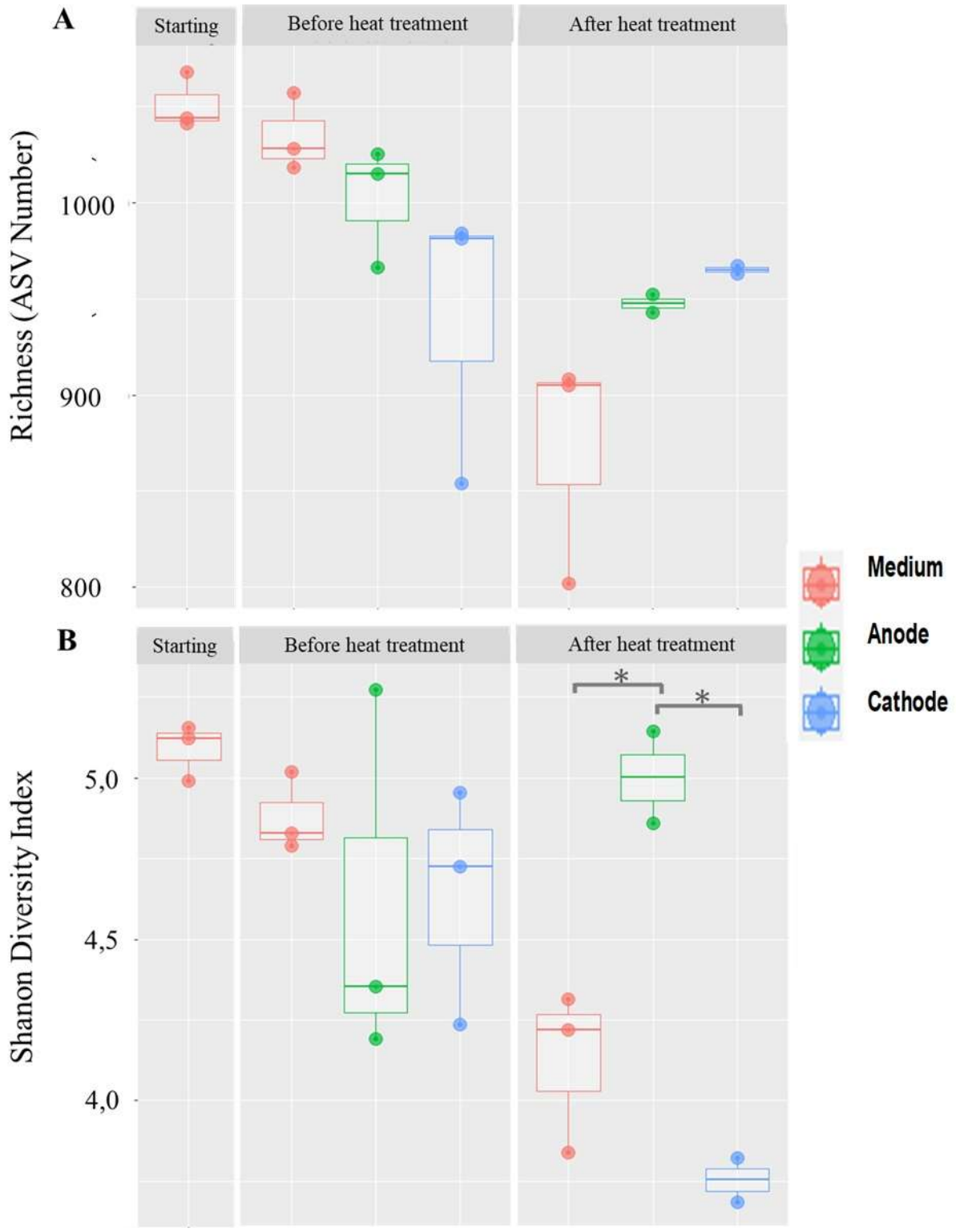
A
Starting
Before heat treatment
After heat treatment
Richness (ASV Number)
1000
900
800
B
Starting
Before heat treatment
After heat treatment
Shanon Diversity Index
5,0
4,5
4,0
*
*
Medium
Anode
Cathode

Figure 7

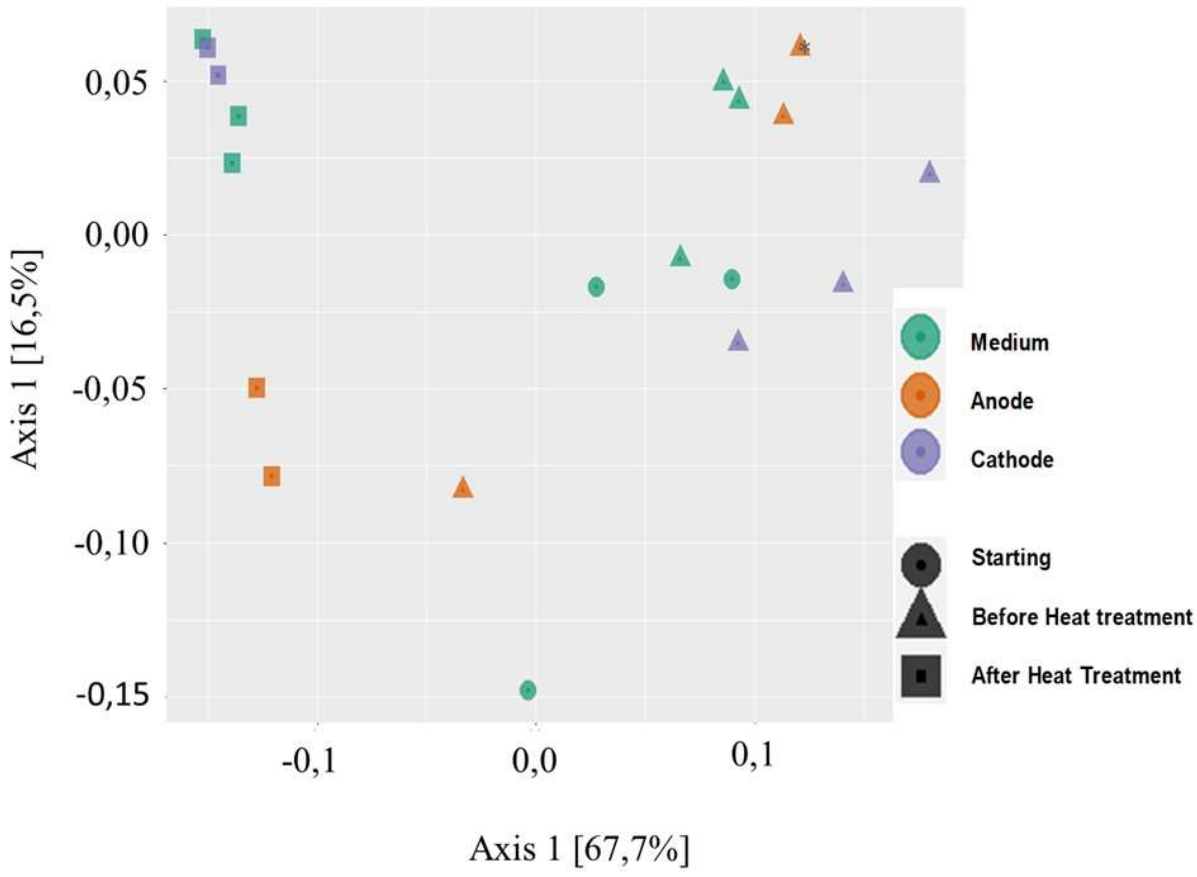
0,05
0,00
-0,05
-0,10
-0,15
Axis 1 [16,5%]
-0,1
0,0
0,1
Axis 1 [67,7%]
Medium
Anode
Cathode
Starting
Before Heat treatment
After Heat Treatment

1

2 Figure 8

3

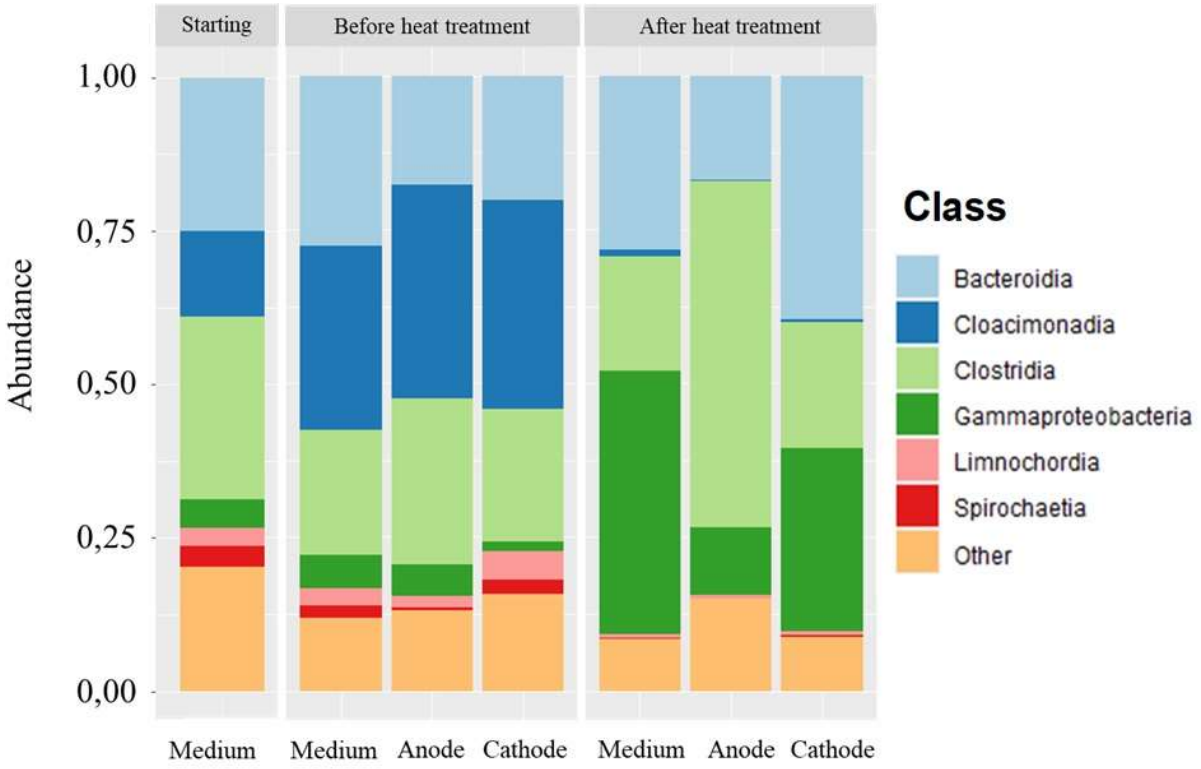
Starting
Before heat treatment
After heat treatment
1,00
0,75
0,50
0,25
0,00
Abundance
Medium
Medium
Anode
Cathode
Medium
Anode
Cathode
Class
Bacteroidia
Cloacimonadia
Clostridia
Gammaproteobacteria
Limnochordia
Spirochaetia
Other

Figure 9

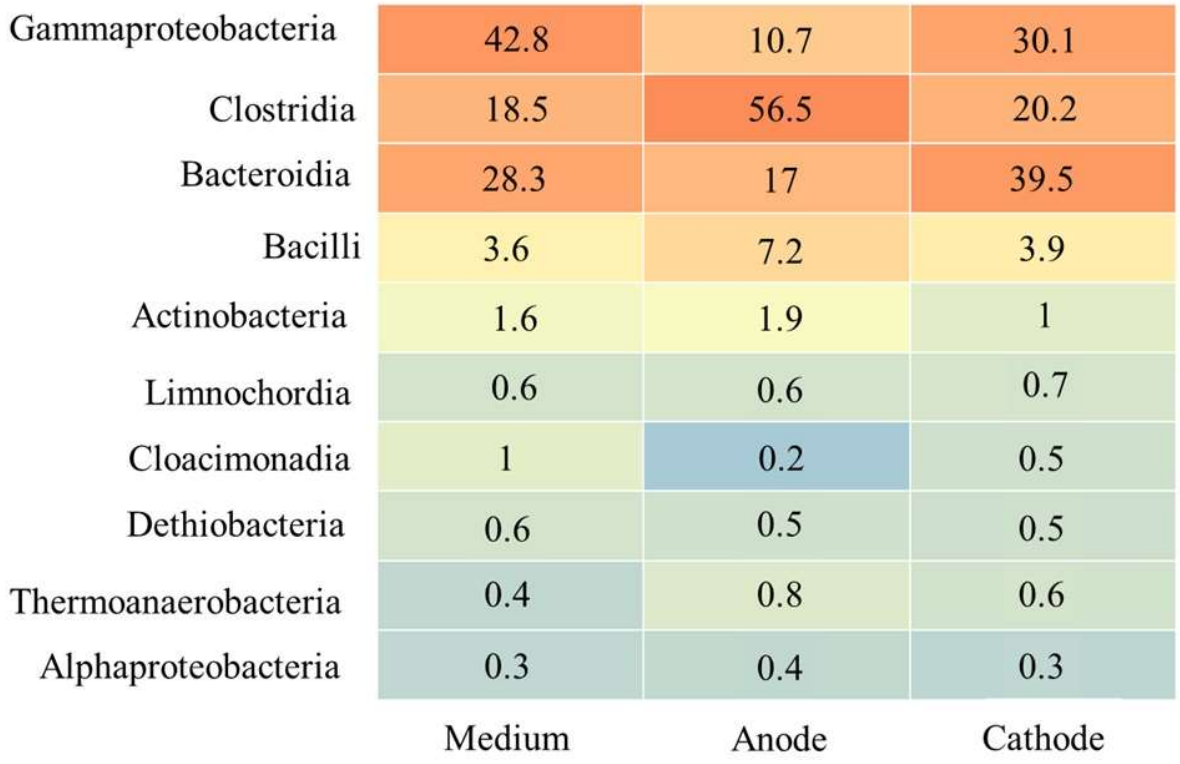

1

2

3 Figure 10

4

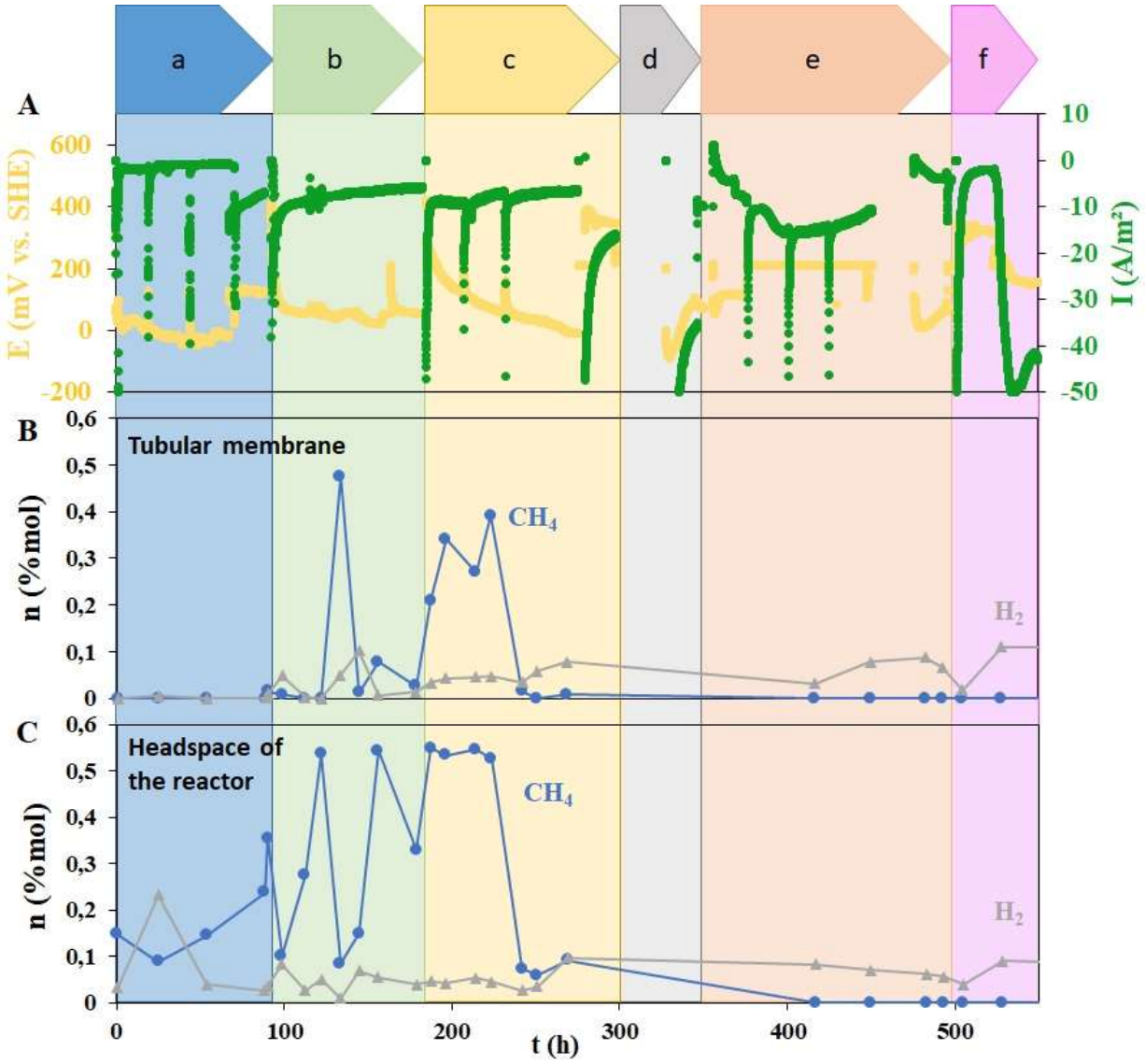
a
b
c
d
e
f
A
E (mV vs. SHE)
I (A/m²)
B
Tubular membrane
CH4
H2
n (%mol)
C
Headspace of the reactor
CH4
H2
n (%mol)
t (h)

Figure A